Investigation of the Stresses and the Deformation in the Laminates Composite Cantilever Beam using Finite Element Analysis

Mohd Saad[1], Dr. Rashmi Dwivedi[2]
[1]M.Tech Scholar, Department of Mechanical Engineering, Sagar Institute of Science &Technology, Bhopal, MP, India
[2]Associate Professor, Department of Mechanical Engineering, Sagar Institute of Science &Technology, Bhopal, MP, India
Email：saadmohd4789@gmail.com, rashmidwivedi@sistec.ac.in

* Corresponding Author: Mohd Saad

Abstract: *In the present work the finite element analysis in order to investigate the stresses and the deformation in the laminates the composite cantilever beam with unidirectional (θ˚/θ˚/θ˚/θ˚) s and angle ply (θ˚/-θ˚/ θ˚/-θ˚) have been used to laminates the composite cantilever beam. Fiber orientation angle θ˚ is varied from 0˚, 15˚, 30˚, 45˚, 60˚, 75˚ and 90˚. A rectangular plate of 100 mm x 50 mm having central hole of 20 mm with total thickness of 1 mm fixed at the left side and the force of 1 KN on the right upper corner has been applied to check the stresses and deformation. For the creation of layer (ply) ACP pre has been used in ansys workbench. The thickness of each layer is taken as 0.125 mm and total eight layers of boron-epoxy are used to make laminate. Results show that the stresses with all orientation of laminated composite cantilever beam, from ply 1 to ply 3 the stress value is decreasing for all orientation and from ply-3 to ply-8 it increasing, it also have been seen that the rectangular laminated composite cantilever beam having the minimum stress value for orientation angle 90o because in this case applied load is along the direction of fiber hence it can be concluded that according to the application of load direction orientation of ply can be make.*

Keywords: Composite Cantilever beam, laminate, stresses and deformation, etc.

I. Introduction

When two or more constituents are united at a macroscopic level and are insoluble in one another, the result is a structural material known as a composite. The matrix refers to both the component in which a constituent is embedded and the reinforcing phase, which is one of them. The material used in the reinforcing phase can take the shape of fibers, particles, or flakes. Materials used in the matrix phase are typically continuous. Concrete reinforced with steel and epoxy reinforced with graphite fibers are two examples of composite systems.

1.1 Classification of Composites

Composites can be categorized by the matrix type (polymer, metal, ceramic, and carbon) or by the geometry of the reinforcement (particulate, flake, or fibers).

Particulate composites are made up of particles that are submerged in matrices like ceramics and alloys. Due to the random addition of the particles, they are typically isotropic. Particulate composites benefit from enhanced strength, higher operating temperature, oxidation resistance, and other benefits. The usage of silicon carbide and aluminium particles, as well as the use of gravel, sand, and cement to create concrete, are typical examples.

• Matrix reinforcements that are flat make up flake composites. Glass, mica, aluminium, and silver are examples of common flake substances. The benefits of flake composites are their inexpensive cost, high out-of-plane flexural modulus, and increased strength. Flakes cannot be easily oriented, though, and there aren't many materials that can be used.

• Matrix-reinforced fiber composites are made of either short (discontinuous) or long (continuous) fibers. Carbon and aramid fibres are two examples of anisotropic fibers. Matrix materials include resins like epoxy, metals like aluminium, and ceramics like calcium-aluminum silicate. This book places a strong emphasis on continuous fiber composites, which are further examined in this chapter by the matrices of polymer, metal, ceramic, and carbon. Unidirectional or woven fiber laminas are the basic building blocks of a continuous fiber matrix composite. A multidirectional laminate is created by stacking laminates on top of one another at different angles.

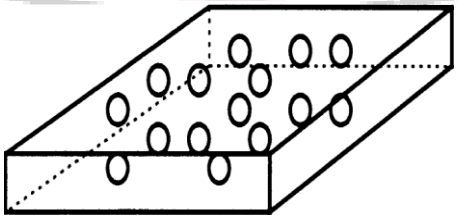

Particulate composites

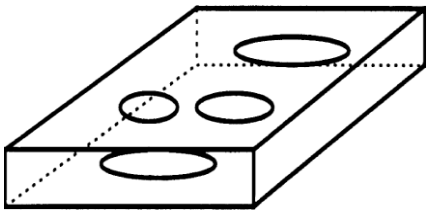

Flake composites

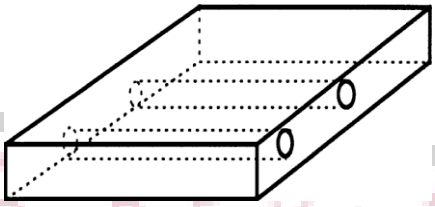

Flake composites

Figure 1 Types of composites based on reinforcement shape.

1.2 Advantages of Composites

The benefit of composites is that they frequently exhibit the best characteristics that neither constituent possesses. One of the properties that may be enhanced by creating a composite material includes;

I. Its high strength to weight ratio, which makes it suitable for aeronautical applications.
II. It has a high rigidity compared to other materials and a high stiffness to weight ratio.
III. Corrosion resistance.
IV. They can be moulded/formed into any desired shape
V. Ability to be customized - The attributes of stiffness and strength can be customized. The ability to tailor a composite material to its job is one of the most Significant advantages of a composite over an ordinary material.
VI. Wear resistance.
VII. Fatigue life.
VIII. Thermal insulation.
IX. Thermal conductivity.
X. Transmission of light
XI. Low maintenance cost – composite materials have low maintenance cost and they have good finishing also.

1.3 Application of Composites

Due to its additional benefits over other conventional materials, composite laminates are frequently used in numerous engineering applications. These are the numerous applications:

I. Aircraft and helicopter application.
II. Space application.
III. Marine application.
IV. Sporting goods application.
V. Electrical application.
VI. Industrial application.
VII. Orthopedic application.
VIII. Constructional application.

1.4 Mechanical behaviors of Composite Material:

Composite material have many characteristics that are different from conventional engineering materials are homogeneous and isotropic.

An isotropic material has properties that are the same in all directions. For example, the Young's modulus of steel is the same in all directions.

A homogeneous body has properties that are the same at all points in the body. A homogenous body is something like a steel rod. However, if one heats this rod from one end, other parts of the rod would have different temperatures. One no longer has a homogenous body since the temperature affects the Young's modulus of steel. Because the properties at a specific point remain the same in all directions, the body is still isotropic. The majority of composite materials are neither homogenous nor isotropic. Take epoxy, for instance, which has been strengthened with long glass fibers. The qualities differ depending on where one decides to place them on the glass fiber vs the epoxy matrix. Because of this, the composite material lacks homogeneity (not homogeneous). Additionally, since the stiffness in the fibers' parallel direction is stronger than that in their perpendicular direction, the properties are not independent of the direction. The composite material becomes anisotropic (not isotropic) as a result.

A nonhomogeneous or inhomogeneous body has non-uniform properties over the body, i.e. the material properties are a function of the position on the body.
An orthotropic body has properties that are different in three mutually perpendicular directions at appoint in the body and, further, have three mutually perpendicular planes of material symmetry. Thus, the properties are a function of orientation at a point in the body.

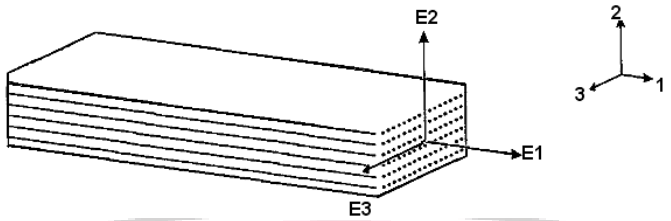

Figure 2 An orthotropic material.

1.5 Advantages Of Fiber Reinforced Composite Materials:
Following are the advantages of fiber-reinforced composite materials:
1. Improved strength(s/p)
2. It has high strength to weight ratio and hence useful in aeronautics applications.
3. Improved stiffness (s/p)
4. It has high rigidity than other materials.
5. This has described properties in different directions.
6. Manufacturing is easy, because no machining is required.
7. These are non-corroding.
8. Formability; they can be formed into any desired shape.
9. Tailor ability; it is possible to tailor the strength and stiffness section.
10. Low maintenance cost; composite materials have low maintenance cost and they have good finishing also.

II. Literature Review

Pascual A et al (2022) [1] In order to investigate the impact of porosity flaws on the mechanical behaviour and failure of L-PBF AlSi10Mg components, this work will provide an XRCT-based FEM methodology. Therefore, using XRCT scanning, measurement of porosity features, and mechanical FEM modelling of digitalized components, the impact of defects on performance is assessed. L-PBF produced certain test specimens with generated artificial porosity in accordance with ASTM E8/E8M for this purpose. Once this was completed, XRCT was used for inspection and defect characterization. In addition to porosity %, other porosity characteristics such as void size, shape, and location were studied. After that, tensile testing and more XRCT inspections were conducted in order to investigate the relationship between the fracture level and the porosity of the as-built sample. Then, with the use of FEM technique, virtual tensile tests of the XRCTed specimens were modelled. The FEM model's predictions of each specimen's ultimate tensile strength and elongation at fracture showed good agreement with the experimental tensile data, with errors under 5.2%. However, the results of the final fracture level predicted by FEM analysis show that there may be defects on the AlSi10Mg specimens that are underestimated or non-detected, which may have an impact on the accuracy of the fracture level prediction in some samples.

Erik Jungstedt et al. (2022) [2] The comparison of nanoscale fibril reinforcement with microscale wood fibers is of interest. Hot-pressed, binder-free wood fiber (WF) composites can be used as load-bearing and eco-friendly materials. Using digital image correlation and orthotropic, elastic-plastic finite element model updating predictions, we examined property differences and interpreted deformation mechanisms with strain field measurements. The intrinsic lignin-hemicellulose binder of random-in-plane microfibrillated lignocellulose (MFLC) composites contributed to improved interfibrillar adhesion and stronger strain-hardening compared to WF composites. When compared to random MFLC, axially oriented wood fiber composites (O-WF) had similar mechanical properties but better eco-indicator values. Despite the plasticity model requiring two more experiments, the FEM updating approach was able to successfully obtain all four independent elastic constants from a single 45° off-axis experiment.

Jun Sun et al. (2022) [3] The steel-concrete composite girder specimen was designed and made in accordance with the existing codes in order to analyze the horizontal shear resistance participation degree of the shear studs on the web and diaphragm flange in the negative moment area of the steel-concrete continuous composite box girder. The stress analysis of the diaphragm and the finite element parameter analysis of the nonlinear shear deformation of the studs are used to study the shear deformation of the two portions of the studs in the composite box girder. The findings demonstrate that web flange studs give the steel-concrete composite box girder its horizontal shear capacity. The shear connection degree of composite beams cannot be increased by the placement of baffle flange studs. Flange stud removal from the diaphragm can relieve the force on the diaphragm and provide a theoretical basis for reducing the stiffners of the diaphragm.

Nan Tao et al. (2022) [4] with heat stress on thick composite materials, this work intends to enhance shearography non-destructive testing (NDT) of deep defects. The main concept is to use novel spatially modulated heating (SMH) for shearography NDT rather than conventional global heating (GH). Shearography has been advanced in this study using the finite element method (FEM) in order to become a quantitative inspection tool for thick composites. For the purpose of assessing their corresponding efficacies in the detection of deep defects, GH and SMH have both been carried out experimentally and modelled in Abaqus. SMH was produced by combining a Fresnel lens on a halogen lamp. A feature that is rarely mentioned in shearography examination, the heat flux distribution on the specimen surface, was taken into account for fault detection.

Tatsuya Doi et al. (2022) [5] In this study, a new composite foundation made of piles and soilbags is proposed, and numerical calculations based on sophisticated models for both soils and structures are used to comprehensively explore its mechanical behaviour. The placement of soilbags between the pile heads and the footing that the superstructure is supported on defines the foundation. In order to reduce the bending moment of the piles and decrease the response acceleration of the structure, the foundation is expected to cut off the fixed junction between the piles and the footing. The proposed composite foundation's seismic response is numerically evaluated in this work using a 3D elastoplastic FEM analysis, and its superiority to the conventional pile foundation is demonstrated in detail. The research reveals that the lengthened natural period of the foundation and increased hysteresis damping of the soilbags decrease both the bending moment and the response acceleration of the pier. The pile's bending moment at the pile heads in the proposed composite foundation is significantly reduced due to the effect of the stress dispersion of the soilbags, in addition to the influence on the response acceleration indicated above.

III. OBJECTIVES

The main objective of this work to perform structure analysis of laminated composite plates with a circular hole in center. There are following objective for this work.

1. To check the total deformation on the laminated composite cantilever beam plates.
2. To check the directional deformation along the X-axis and Y-axis of the laminated composite cantilever beam plates.
3. To check the equivalent stress on different ply for all the orientation of the laminated composite cantilever beam plates.
4. Compare the results obtained after the structure analysis with all parameters.

IV. METHODOLOGY

4.1 Mechanics of Laminate

The major distinction between a laminate and a lamina is that a laminate is made by stacking several of these thin layers of composite material in the direction of the lamina thickness. These laminates are used to create mechanical structures that are subjected to loads like twisting and bending. Understanding the stresses and strains in the laminate is necessary for the design and analysis of such laminated structures. The values of these laminate stresses and strains are also required by design tools like stiffness models and failure theories. Comprehending a laminate requires understanding a lamina's mechanical analysis first. An isotropic homogeneous material is not a lamina. For instance, the stiffness of the lamina varies from point to point depending on whether the point is in the fiber, the matrix, or the interface between the fiber and the matrix if the lamina is formed of an isotropic homogeneous matrix. Any mechanical modelling of the lamina will be extremely difficult to complete without taking into account these variances. Because of this, a lamina's micromechanical analysis relies on average properties and assumes that the lamina is homogeneous.

4.2 Classical Laminate Theory

The classical lamination theory is used to develop these relationships. The following assumptions are made in the classical lamination theory to develop the relationships

- Each lamina is orthotropic.
- Each lamina is homogeneous.
- A line straight and perpendicular to the middle surface remains straight and perpendicular to the middle surface during deformation ($\gamma_{xz}= \gamma_{yz}= 0$).
- The laminate is thin and is loaded only in its plane (plane stress) ($\sigma_x= \tau_{xz}=\tau_{yz} = 0$).
- Displacements are continuous and small throughout the laminate ($|u|,|v|,|w|<<|h|$) , where h is the laminate thickness
- Each lamina is elastic.
- No slip occurs between the lamina interfaces.

Consider a side view of a plate in the Cartesian *x–y–z*
Coordinate system. The origin of the plate is at the midplane of the plate, that is, $z= 0$. Assume u_0, v_0, and w_0 to be displacements in the *x*, *y*, and *z*. directions, respectively, at the midplane and *u*,*v*, and *w*here the displacements at any point in the *x* , *y* , and *z* directions, respectively. At any point other than the midplane,

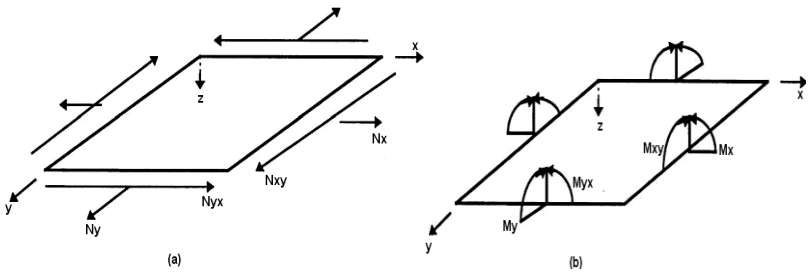

Figure 3 Resultant force and moment on a laminate

the two displacements in the *x*–*y* plane will depend on the axial location of the point and the slope of the laminate midplane with the *x* and *y* directions.

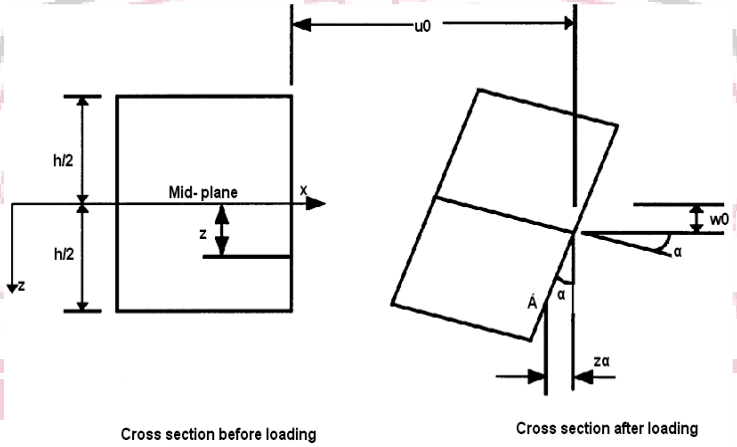

Figure 4 Relationship between displacements through the thickness of a plate to midplane displacements and curvatures

$$u = u_0 - z\alpha$$

$$\alpha = \frac{\partial W0}{\partial x}$$

Thus, the displacement *u* in the x direction is

$$u = u_0 - z\frac{\partial W0}{\partial x}.$$

Similarly, taking a cross-section in the *y*–*z* plane would give the displacement in the *y* -direction as

$$v = v_0 - z\frac{\partial W0}{\partial x}.$$

$$\varepsilon_x = \frac{\partial u}{\partial x} = \frac{\partial U0}{\partial x} - z\frac{\partial^2 W0}{\partial x^2}$$

$$\varepsilon_y = \frac{\partial v}{\partial x} = \frac{\partial V0}{\partial x} - z\frac{\partial^2 W0}{\partial x^2}$$

$$\gamma_{xy} = \frac{\partial u}{\partial x} + \frac{\partial v}{\partial x} = \frac{\partial U0}{\partial x} + \frac{\partial V0}{\partial x} - 2z\frac{\partial^2 W0}{\partial x^2}$$

The strain-displacement equations can be written in matrix form as

$$\begin{bmatrix} \varepsilon_x \\ \varepsilon_y \\ \gamma_{xy} \end{bmatrix} = \begin{bmatrix} \frac{\partial U0}{\partial x} \\ \frac{\partial V0}{\partial x} \\ \frac{\partial U0}{\partial x} + \frac{\partial V0}{\partial x} \end{bmatrix} + Z \begin{bmatrix} -\frac{\partial^2 W0}{\partial x^2} \\ -\frac{\partial^2 W0}{\partial y^2} \\ -2\frac{\partial^2 W0}{\partial x \partial y} \end{bmatrix}$$

the midplane strains:

$$\begin{bmatrix} \varepsilon^{0}_{x} \\ \varepsilon^{0}_{y} \\ \gamma^{0}_{xy} \end{bmatrix} = \begin{bmatrix} \dfrac{\partial U0}{\partial x} \\ \dfrac{\partial V0}{\partial x} \\ \dfrac{\partial U0}{\partial x} + \dfrac{\partial V0}{\partial x} \end{bmatrix}$$

and the midplane curvatures

$$\begin{bmatrix} \kappa_x \\ \kappa_y \\ \kappa_{xy} \end{bmatrix} = \begin{bmatrix} -\dfrac{\partial^2 W0}{\partial x^2} \\ -\dfrac{\partial^2 W0}{\partial y^2} \\ -2\dfrac{\partial^2 W0}{\partial x \partial y} \end{bmatrix}$$ respectively,

Therefore, the laminate strains can be written as

$$\begin{bmatrix} \varepsilon_x \\ \varepsilon_y \\ \gamma_{xy} \end{bmatrix} = \begin{bmatrix} \varepsilon^{0}_{x} \\ \varepsilon^{0}_{y} \\ \gamma^{0}_{xy} \end{bmatrix} + Z \begin{bmatrix} \kappa_x \\ \kappa_y \\ \kappa_{xy} \end{bmatrix}$$

(a) Strain and Stress in a Laminate

The global stresses in each lamina:

$$\begin{bmatrix} \sigma_x \\ \sigma_y \\ \tau_{xy} \end{bmatrix}_k = \begin{bmatrix} \overline{Q}_{11} & \overline{Q}_{12} & \overline{Q}_{16} \\ \overline{Q}_{12} & \overline{Q}_{22} & \overline{Q}_{16} \\ \overline{Q}_{16} & \overline{Q}_{26} & \overline{Q}_{66} \end{bmatrix}_k \begin{bmatrix} \varepsilon_x \\ \varepsilon_x \\ \gamma_{xy} \end{bmatrix}_k$$

The reduced transformed stiffness matrix $\overline{Q}$ corresponds to that of the ply located at the point along the thickness of the laminate.

$$\begin{bmatrix} \sigma_x \\ \sigma_y \\ \tau_{xy} \end{bmatrix}_k = \begin{bmatrix} \overline{Q}_{11} & \overline{Q}_{12} & \overline{Q}_{16} \\ \overline{Q}_{12} & \overline{Q}_{22} & \overline{Q}_{16} \\ \overline{Q}_{16} & \overline{Q}_{26} & \overline{Q}_{66} \end{bmatrix}_k \begin{bmatrix} \varepsilon^{0}_{x} \\ \varepsilon^{0}_{y} \\ \gamma^{0}_{xy} \end{bmatrix}_k + z \begin{bmatrix} \overline{Q}_{11} & \overline{Q}_{12} & \overline{Q}_{16} \\ \overline{Q}_{12} & \overline{Q}_{22} & \overline{Q}_{16} \\ \overline{Q}_{16} & \overline{Q}_{26} & \overline{Q}_{66} \end{bmatrix}_k \begin{bmatrix} \kappa_x \\ \kappa_y \\ \kappa_{xy} \end{bmatrix}$$

(b) Finite element analysis:

It's a relatively new idea to use finite element analysis as a tool to solve different engineering challenges in industrial applications. Additionally, it is used in calculations, simulations, and models to forecast and comprehend how an object might react under certain physical circumstances.

4.3 ANSYS Capabilities:

In FEM (finite element analysis) ANSYS software is used that helps engineers for performing the following works:

- To build computer prototype, components, transfer CAD model structures in a system products.
- Enhances the profile of structural member with shape optimization.
- To study stress levels, temperature distributions.
- To reduce production costs design should be optimized in early development process.
- Testing of prototypes is done in normal condition where it otherwise would be undesirable or impossible (for example, biomedical applications).

Graphical user interface (GUI) in ANSYS gives users an easy, interactive approach to documentation, program functions, commands, and reference material. To navigate through the ANSYS program an intuitive menu system is used by users. Input data can be given using a mouse, a keyboard, or a combination of both.

Analysis Steps in ANSYS:

The different analysis steps involved in ANSYS are mentioned below.

I. Preprocessor

The model setup is basically done in preprocessor. The different steps in pre-processing are

- Build the model
- Define materials
- Generation of element mesh

II. Solution Processor

Here, the issue is fixed by compiling all necessary information about the issue. The instant equation produced by the finite element approach is solved by the computer during this phase of the analysis. The nodal degree of freedom values obtained from the solution define the initial solution derived values that shapes the component.

III. Postprocessor

The general postprocessor is where the analysis results are reviewed over the entire model. The potential of the postprocessor range from graphic displays and tabular listings to more complex information manipulations, such as the combining of load cases.

4.4 Algorithm used for Finite Element analysis:

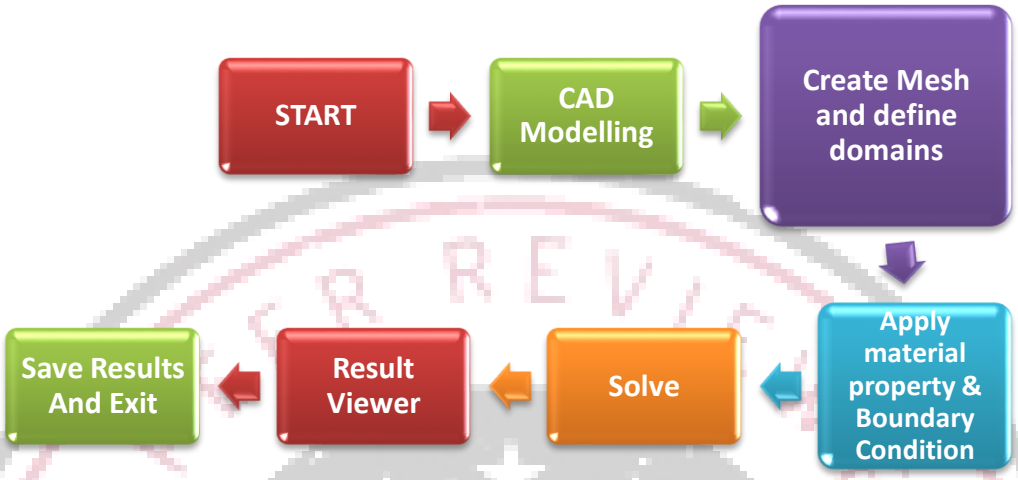

Figure 5 Algorithm used for Finite Element analysis

4.5 CAD modeling:

The two dimensional CAD model of laminated composite cantilever beam with hole in center has been created in ACP pre of ANSYS workbench with the length of 100 mm and the width of the laminated part is 50 mm and a circular hole of 20 mm in diameter placed at the center of the laminated composite cantilever beam (distance from fixed support 50 mm in X-direction and 25 mm in Y-direction) as shown in figure.

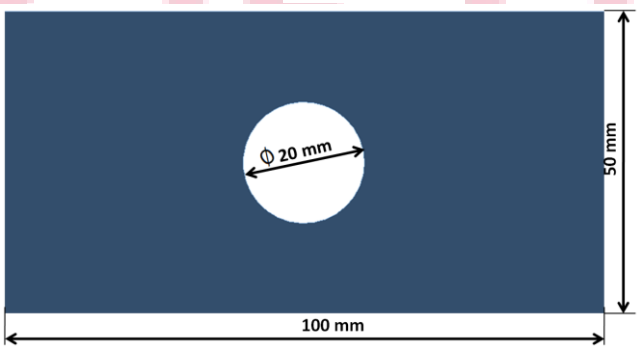

Figure 6 Two dimensional CAD model of laminated composite cantilever beam with hole in center

Meshing: After the creation of CAD model, the next step is meshing, meshing is a critical operation in which CAD model is divided into small pieces of elements or discretization of CAD geometry. In the present work total, no. of nodes is 19280 and the total number of elements is 18922 having quadrilateral elements as shown in figure.

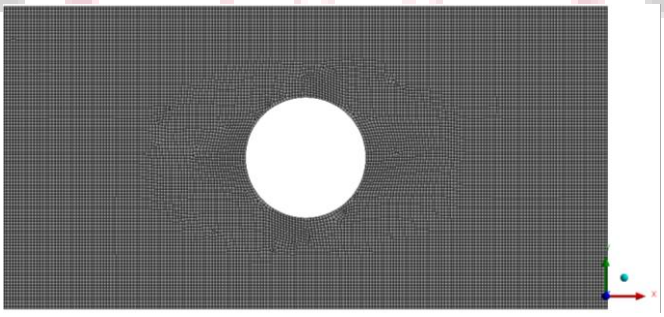

Figure 7 Meshing of laminated composite cantilever beam with hole in center

Stacup Orientation (Fiber direction) of ply at different angles:

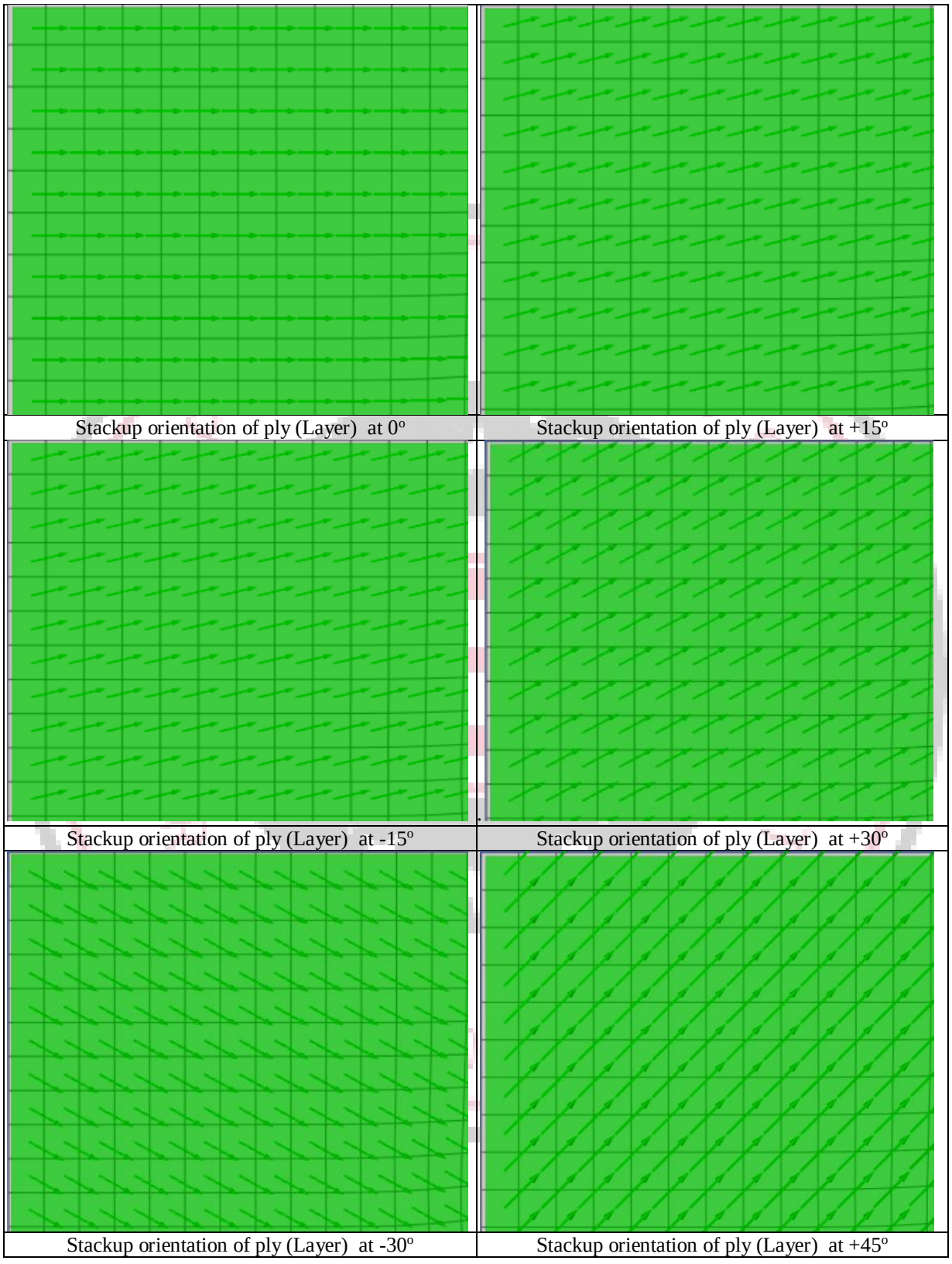

Stackup orientation of ply (Layer) at 0º

Stackup orientation of ply (Layer) at +15º

Stackup orientation of ply (Layer) at -15º

Stackup orientation of ply (Layer) at +30º

Stackup orientation of ply (Layer) at -30º

Stackup orientation of ply (Layer) at +45º

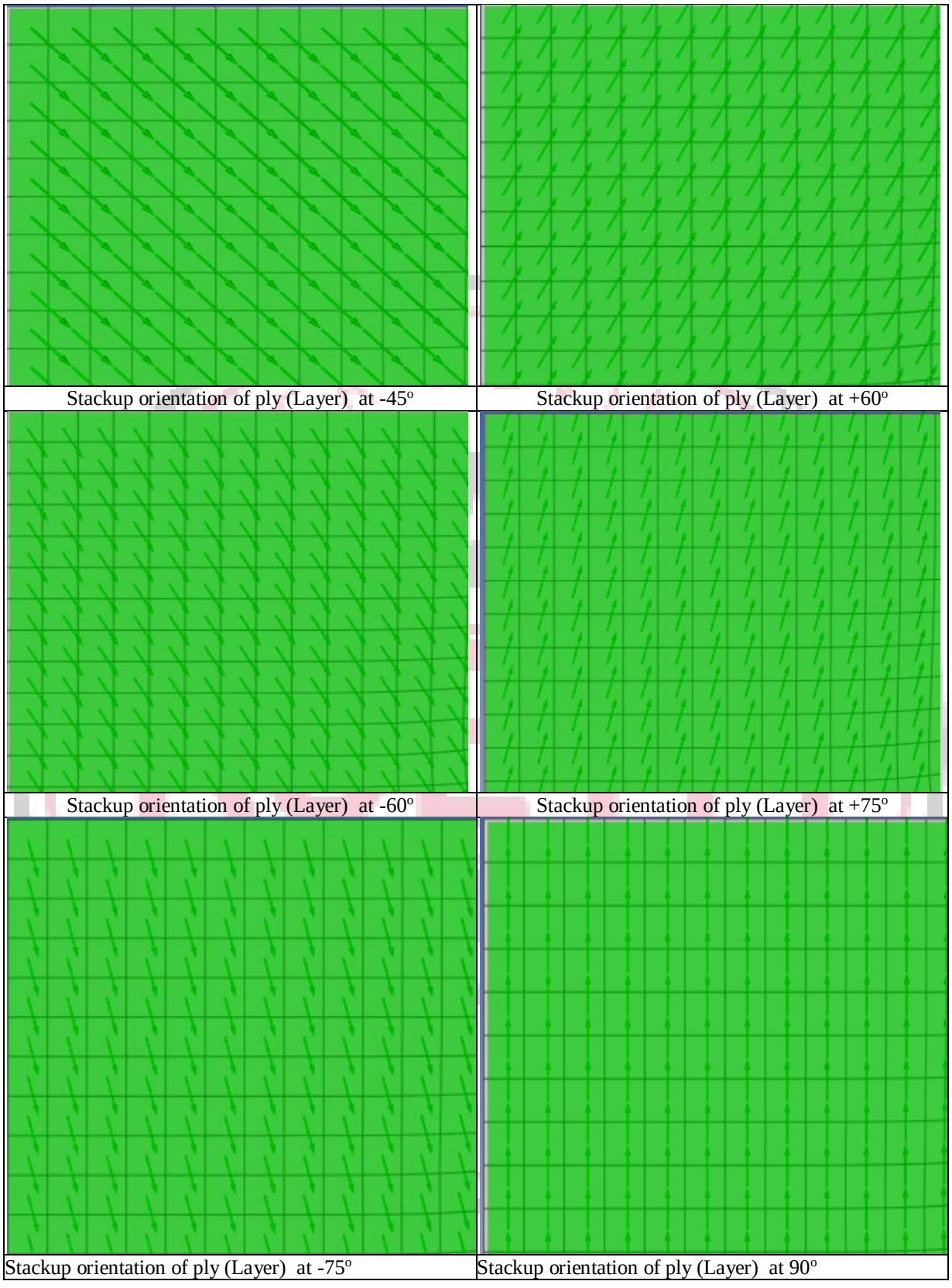

Figure 8 Stacup Orientation of ply at different angles

Table 1 Material property of the boron/epoxy lamina *[P. Uniyal & A. Misra (2016)]*

Parameters	Value with Units
Ex	204 Gpa
Ey	185 Gpa
Vxy	0.23
Gxy	5.59 Gpa
Xt	1260 Mpa
Xc	2500 Mpa
Yt	61 Mpa
Yc	202 Mpa
S	67 MPa

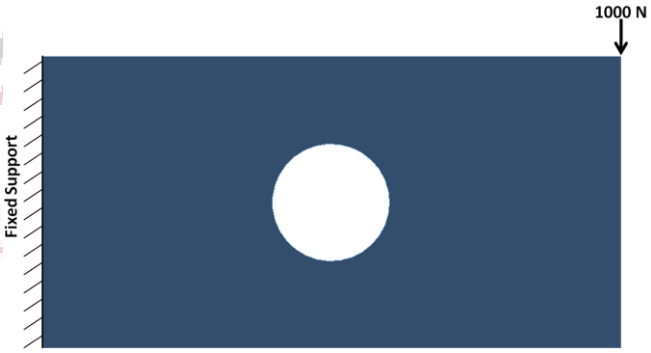

Figure 9 Cantilever beam with stress concentration subjected to point load

4.6 Boundary Conditions

1. For the creation of rectangular laminates the composite cantilever beam ACP-pre is use where laminates has been created by combining two or more layered materials.
2. Create material library for boron-epoxy, the thickness of each layer is taken as 0.125 mm and total eight layers used to make laminate.
3. Apply material for the creation of layers for rectangular laminates the composite cantilever beam.
4. Apply different orientation 0˚, 15˚, 30˚, 45˚, 60˚, 75˚ and 90˚ of layers and rosette with 0.125 mm thickness.
5. Create modelling group in and set eight ply in group with different orientation such as for unidirectional (θ˚/θ˚/θ˚/θ˚) s and for angle ply (θ˚/-θ˚/ θ˚/-θ˚).
6. Convert all ply in one solid for the further structure, analysis and then imported for meshing of rectangular laminates the composite cantilever beam.
7. Create mesh with total no of nodes 19280 and total no. of elements 18922 for the element size 0.5 mm having quadrilateral elements.
8. For the structural analysis by keep left side fixed and applies a compressive load of 1 KN on right top corner of the rectangular laminates the composite cantilever beam. *[P. Uniyal & A. Misra (2016)]*

4.7 Grid independent test

Grid independence has a direct impact on the truncation error or even the rationality of numerical results, and it is related to the correctness of numerical results. An extremely dense grid can prevent this issue when considering grid-independent test, but the calculation resource might be lost unnecessarily. In practice, we often compare the outcomes of two neighborhoods after increasing the grid resolution in accordance with a predetermined ratio. The grid can be regarded as grid-independent if the outcomes tend to be identical. Such an approach can produce reasonable outcomes while utilizing computational resources as effectively as possible.

In the present work finite element analysis have been conducted on the laminates the composite cantilever beam with unidirectional (θ˚/θ˚/θ˚/θ˚) s and angle ply (θ˚/-θ˚/ θ˚/-θ˚) have been used to laminates the composite cantilever beam. A rectangular plate of 100 mm x 50 mm having central hole of 20 mm with total thickness of 1 mm fixed at the left side and the force of 1 KN on the right upper corner has been applied to check the stresses and deformation. The grid independent test performed at 1 KN compressive load in order to check the total deformation and equivalent stress in order to check how numerical result converges with refining of grid as shown in figure.

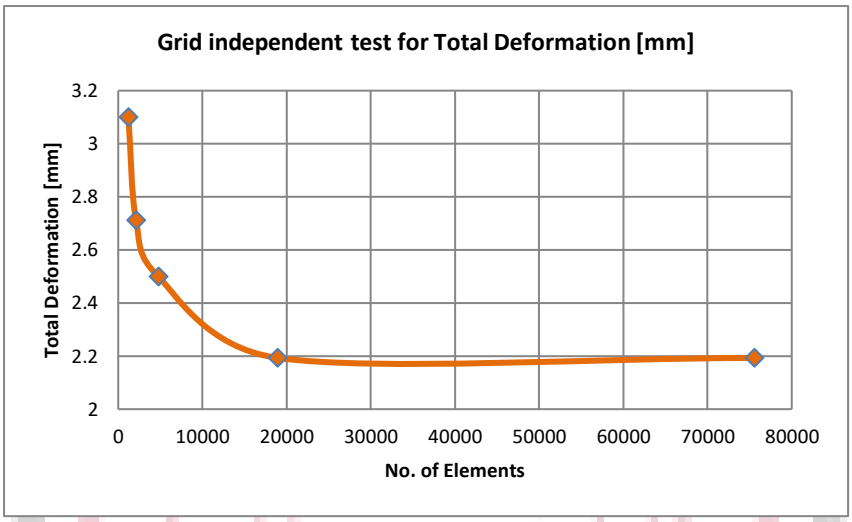

Figure 10 Grid independent test for total deformation

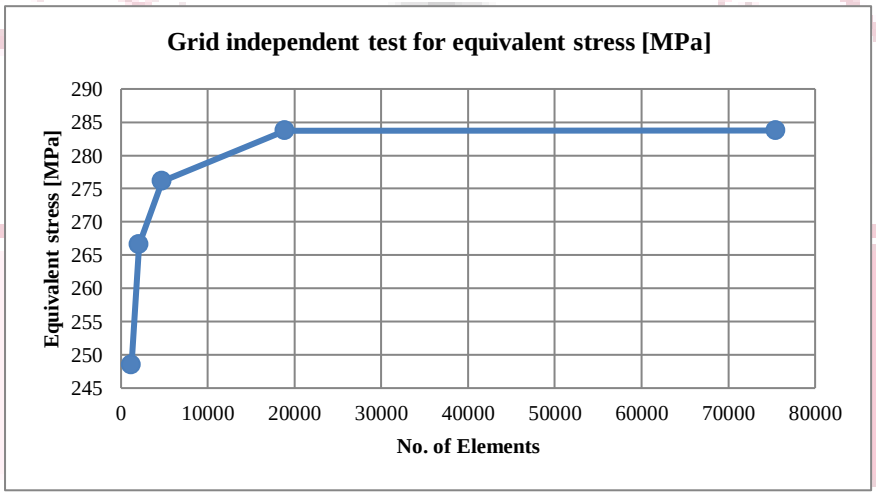

Figure 11 Grid independent test for equivalent stress

V. RESULTS

In the present work the finite element analysis in order to investigate the stresses and the deformation in the laminates the composite cantilever beam with unidirectional (θ˚/θ˚/θ˚/θ˚) s and angle ply (θ˚/-θ˚/ θ˚/-θ˚) have been used to laminates the composite cantilever beam. Fiber orientation angle θ˚ is varied from 0˚, 15˚, 30˚, 45˚, 60˚, 75˚ and 90˚. To test the stresses and deformation, a 100 mm x 50 mm rectangular plate with a 20 mm central hole and a total thickness of 1 mm was attached at the left side and given a 1 KN force on the right upper corner. In the Ansys workbench, ACP pre has been used to create layer (ply). Each layer is assumed to be 0.125 mm thick, and a total of eight boron-epoxy layers are utilized to create the laminate. This chapter uses counters and graphs to discuss various outcomes from the finite element analysis.

5.1 Finite Element Analysis for the ply orientation at 0º

The composite cantilever beam at 1000 N applied in the vertical direction for the ply orientation at 0˚ underwent total deformation of 13.534 mm after structural study on rectangular laminates, as shown in the figure.

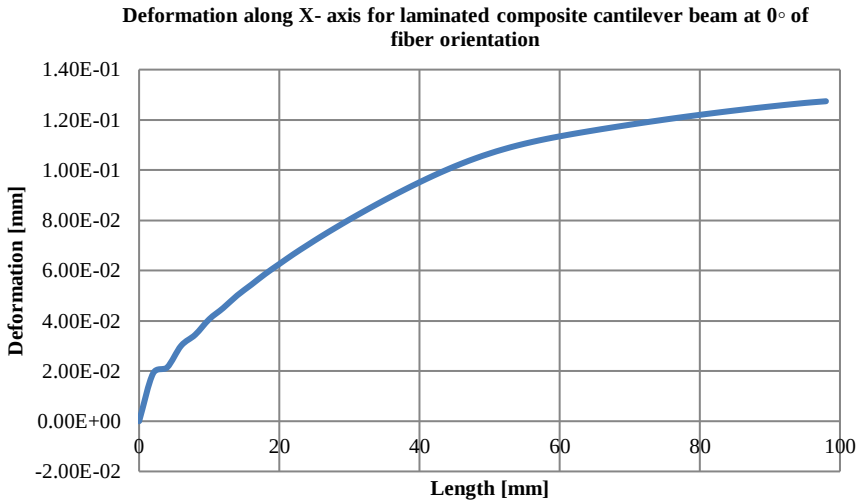

Figure 12 Deformation along X- axis for laminated composite cantilever beam at 0˚ of fiber orientation

At zero degrees of fiber orientation, the graph above depicts the deformation along the X-axis for a laminated composite cantilever beam. It has been noted that the deformation increases along the axis up to a maximum of 0.12759 mm at the maximum length of the laminated composite cantilever beam.
At 0˚ of fiber orientation, Figure 13 depicts the deformation along the Y-axis for a laminated composite cantilever beam. It has been noted that the deformation increases up to 25 mm in length before reducing for the remaining length of the vertical laminates along the axis. At 25 mm in length, the deformation's maximum value is 1.0608 mm.

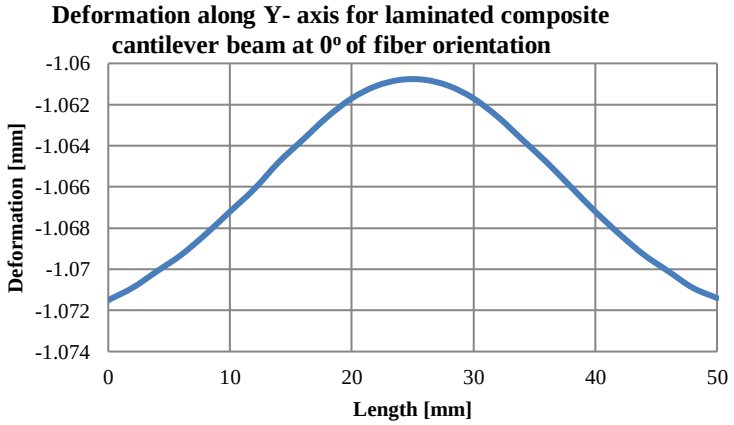

Figure 13 Deformation along Y- axis for laminated composite cantilever beam at 0º of fiber orientation

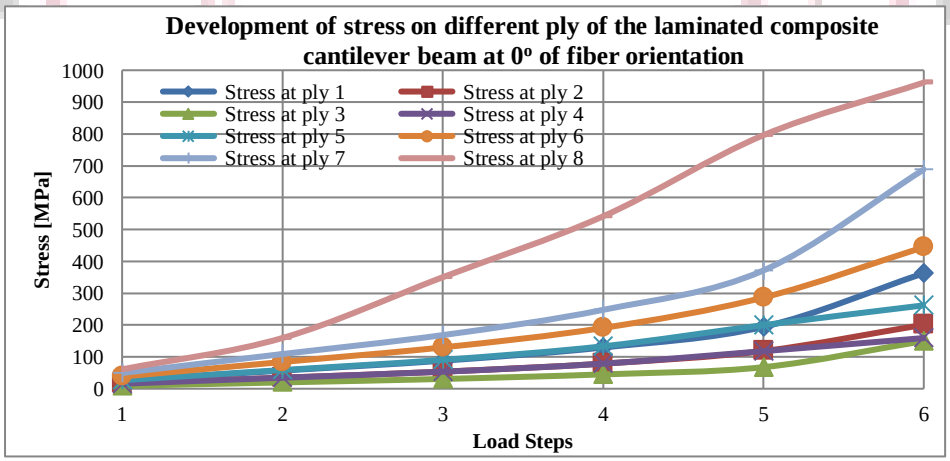

Figure 14 Development of stress on different ply of the laminated composite cantilever beam at 0º of fiber orientation

Figure shows the generation of stress on different ply of the laminated composite cantilever beam at 0º of fiber orientation, it has been observed that the maximum stress of 961.32 MPa generated on 8th ply while the minimum stress of 149.73 MPa on the 3rd ply.

5.2 Finite Element Analysis for the ply orientation at 15º

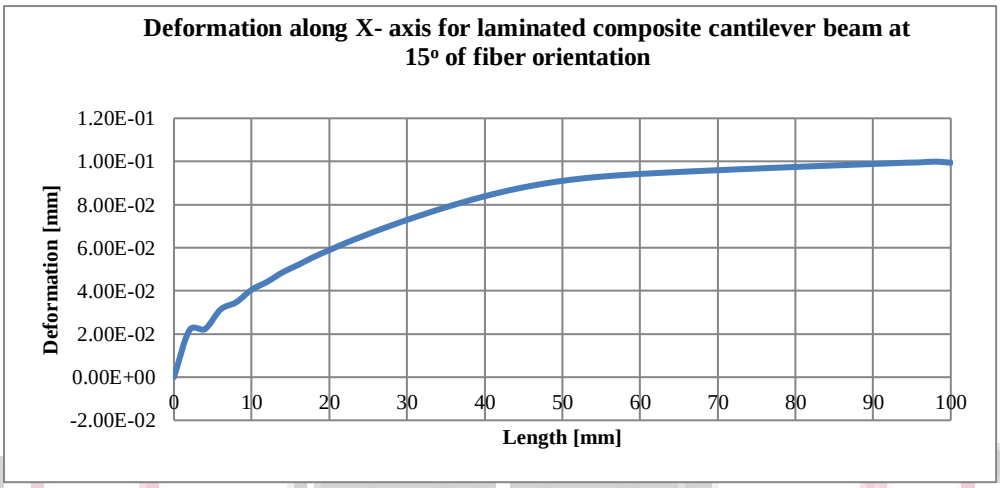

Figure 15 Deformation along X- axis for laminated composite cantilever beam at 15º of fiber orientation

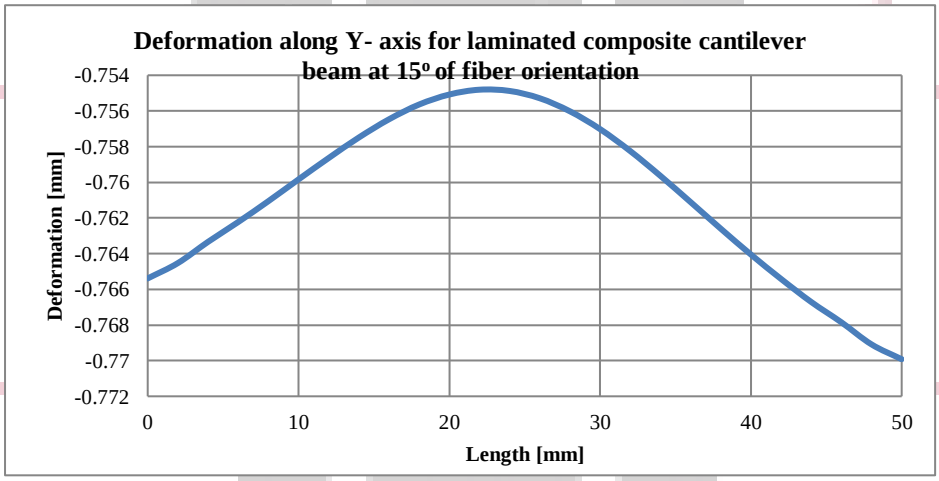

Figure 16 Deformation along Y- axis for laminated composite cantilever beam at 15º of fiber orientation

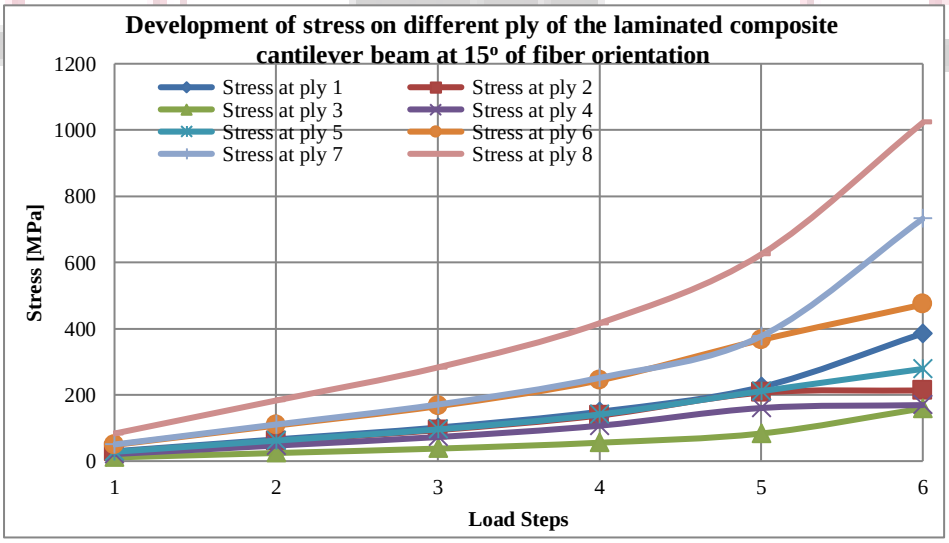

Figure 17 Development of stress on different ply of the laminated composite cantilever beam at 15º of fiber orientation

5.3 Finite Element Analysis for the ply orientation at 30º

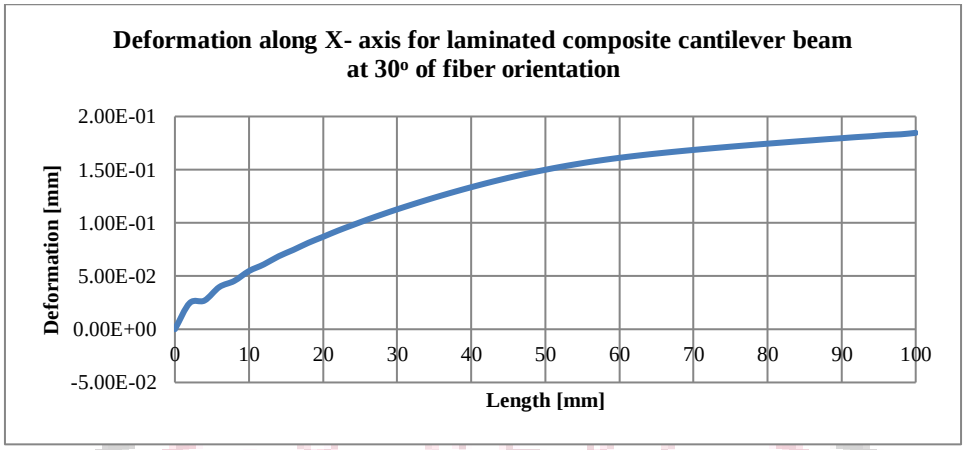

Figure 18 Deformation along X- axis for laminated composite cantilever beam at 30º of fiber orientation

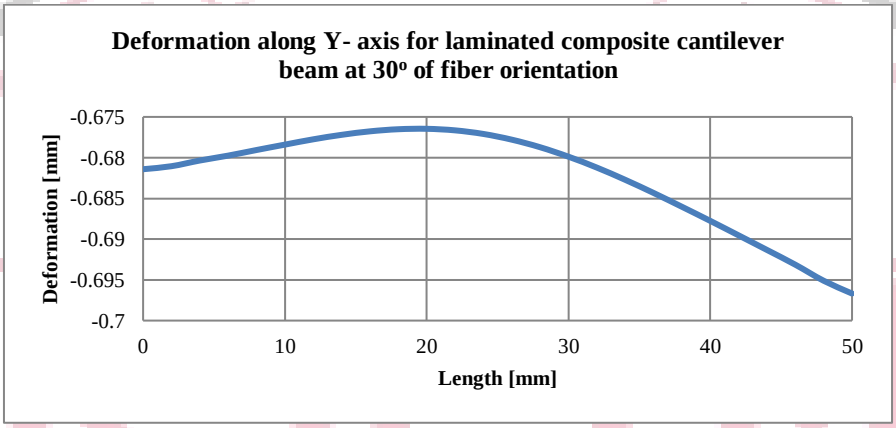

Figure 19 Deformation along Y- axis for laminated composite cantilever beam at 30º of fiber orientation

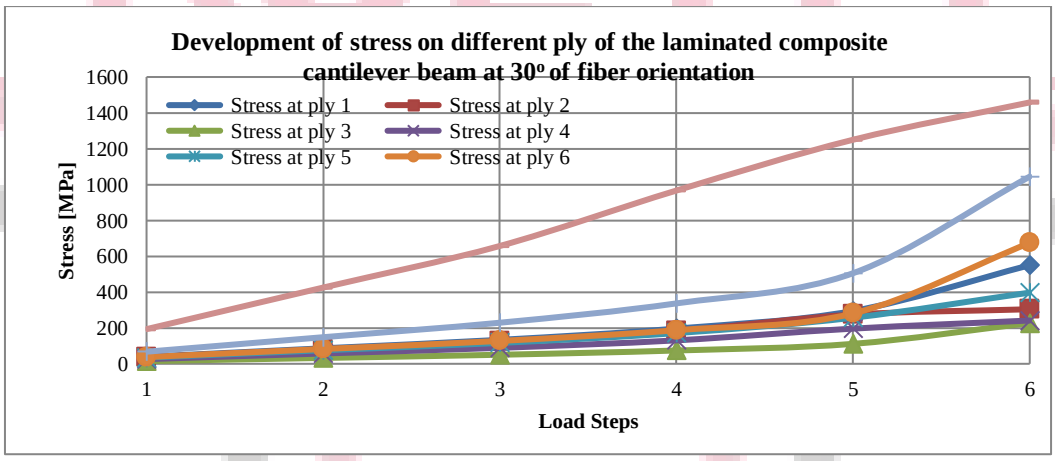

Figure 20 Development of stress on different ply of the laminated composite cantilever beam at 30º of fiber orientation

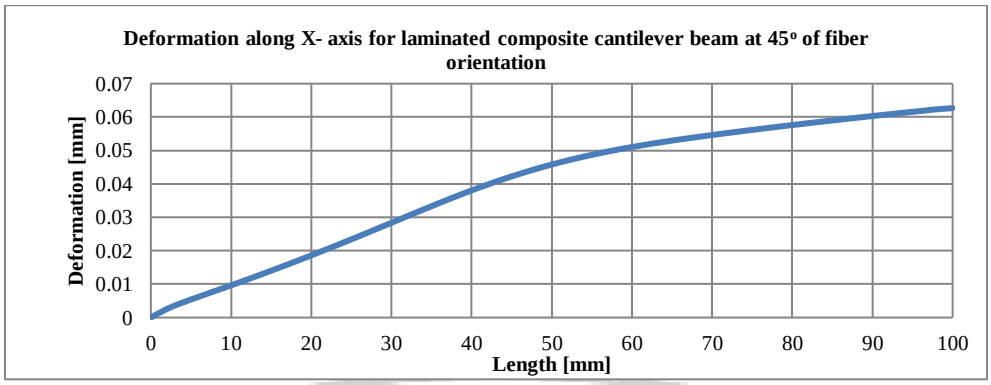

Figure 21 Deformation along X- axis for laminated composite cantilever beam at 45° of fiber orientation

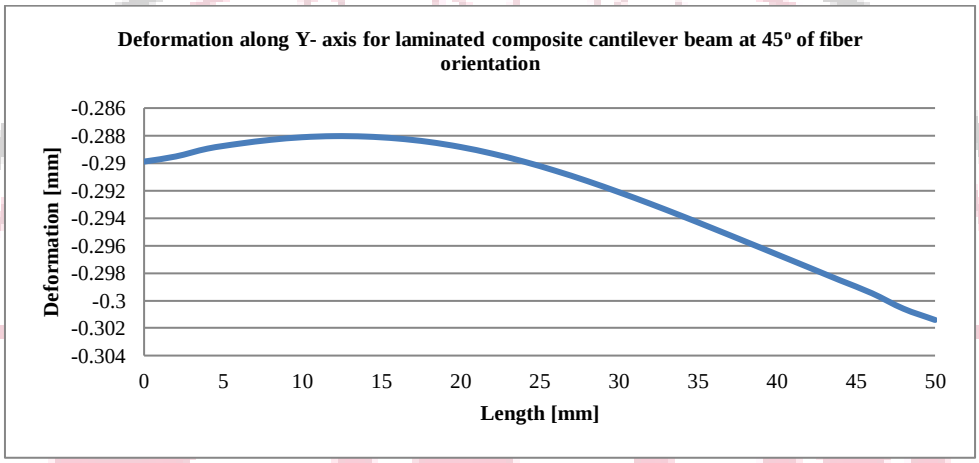

Figure 22 Deformation along Y- axis for laminated composite cantilever beam at 45° of fiber orientation

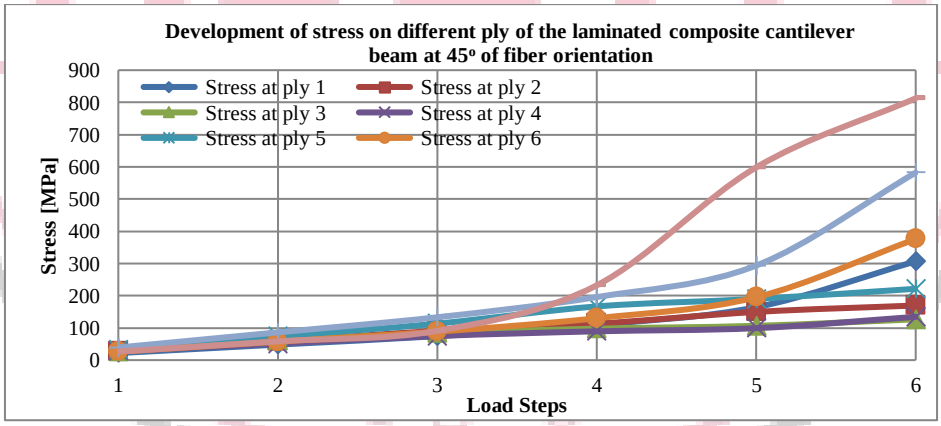

Figure 23 Development of stress on different ply of the laminated composite cantilever beam at 45° of fiber orientation

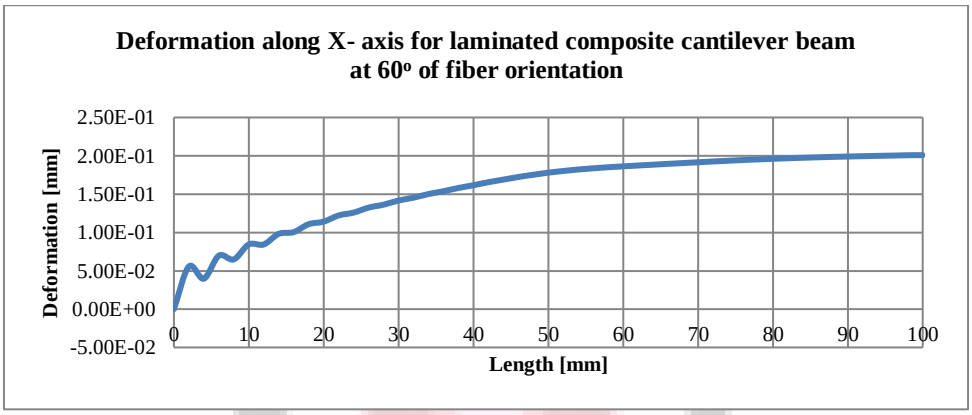

Figure 24 Deformation along X- axis for laminated composite cantilever beam at 60º of fiber orientation

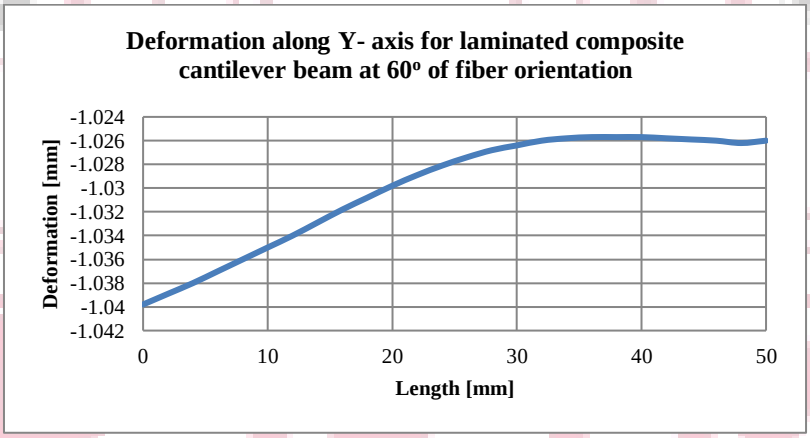

Figure 25 Deformation along Y- axis for laminated composite cantilever beam at 60º of fiber orientation

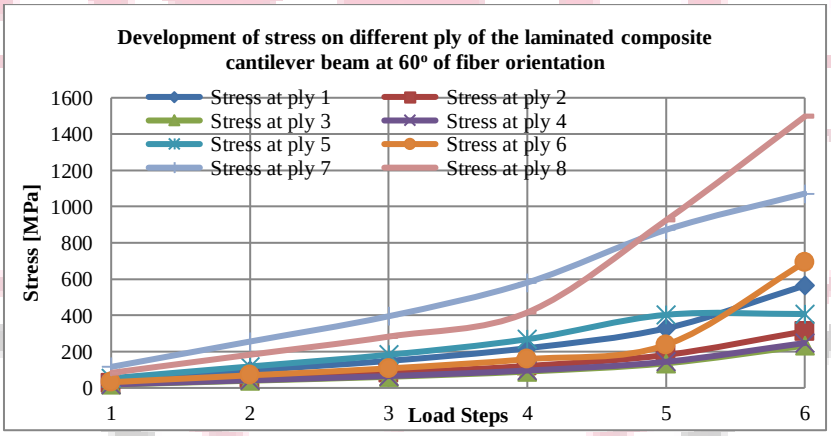

Figure 26 Development of stress on different ply of the laminated composite cantilever beam at 60º of fiber orientation

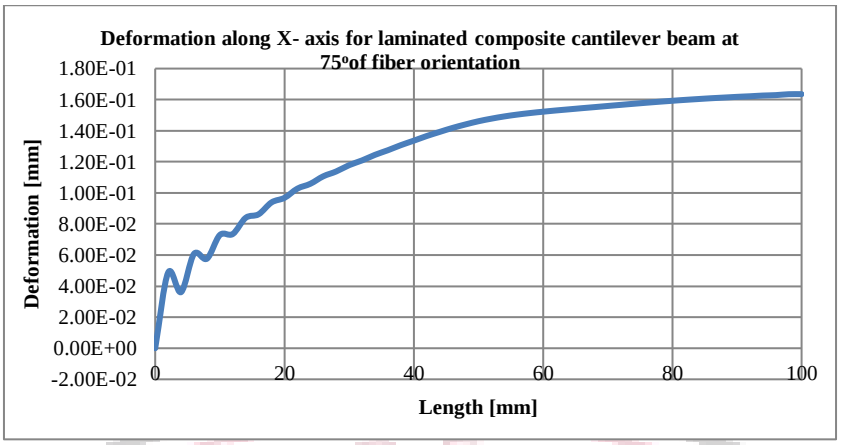

Figure 27 Deformation along X- axis for laminated composite cantilever beam at 75º of fiber orientation

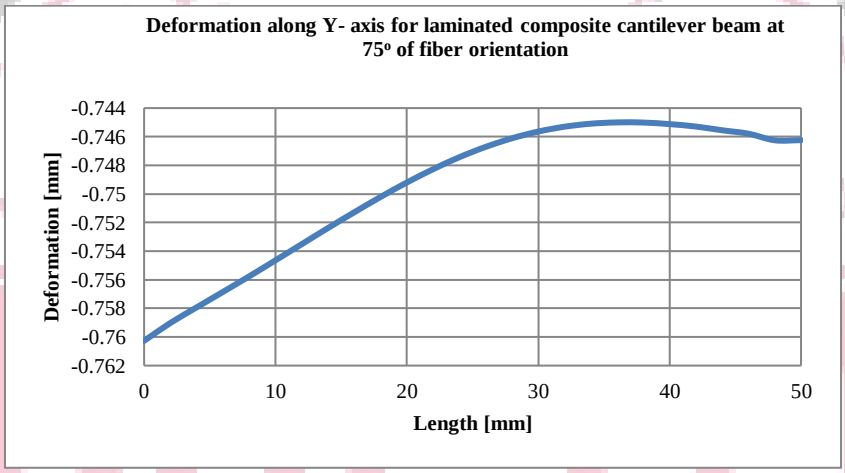

Figure 28 Deformation along Y- axis for laminated composite cantilever beam at 75º of fiber orientation

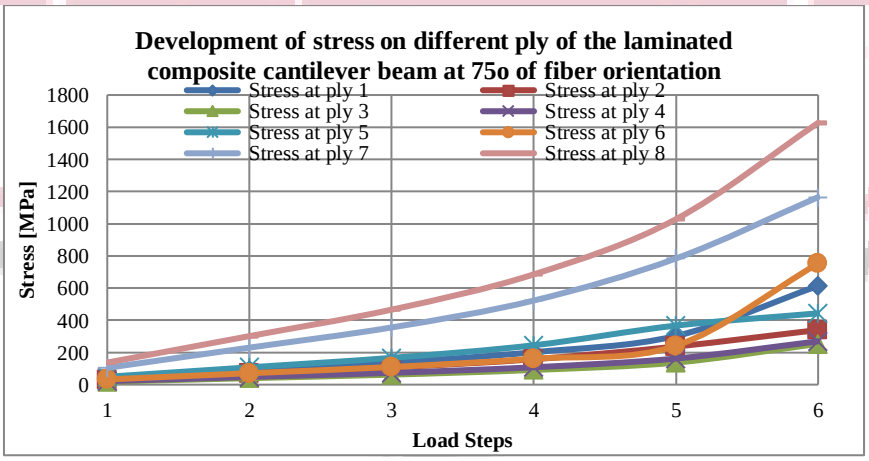

Figure 29 Development of stress on different ply of the laminated composite cantilever beam at 75 º of fiber orientation

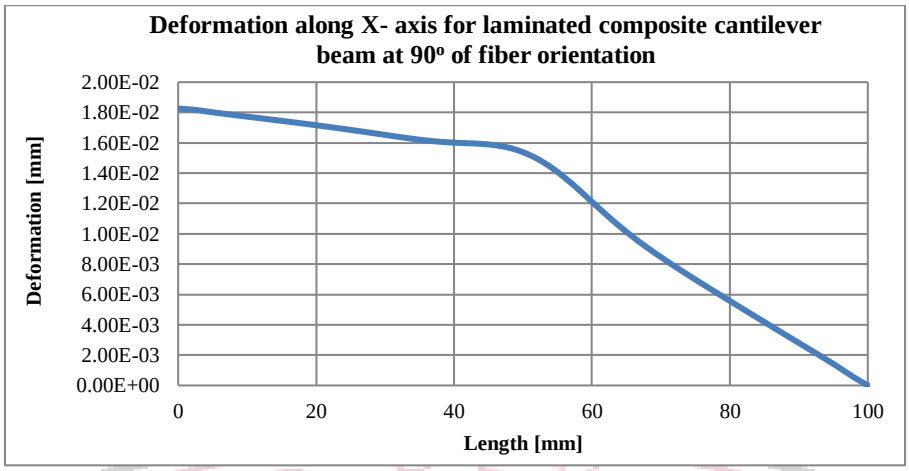

Figure 30 Deformation along X- axis for laminated composite cantilever beam at 90º of fiber orientation

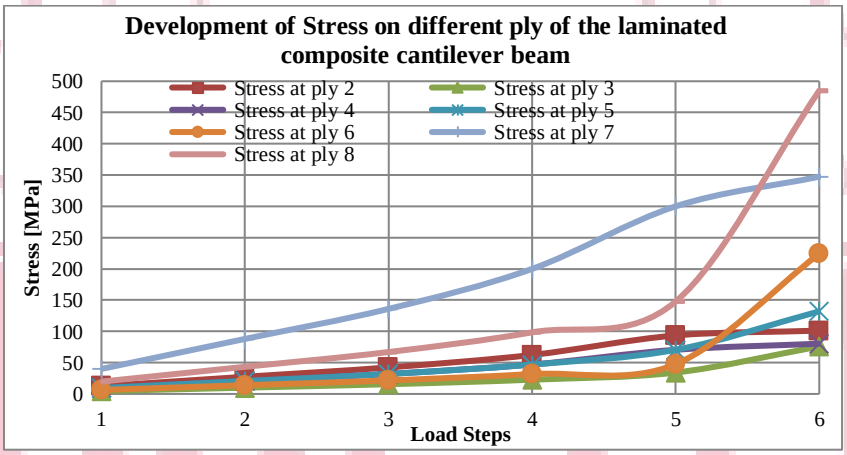

Figure 31 Development of stress on different ply of the laminated composite cantilever beam at 90º of fiber orientation

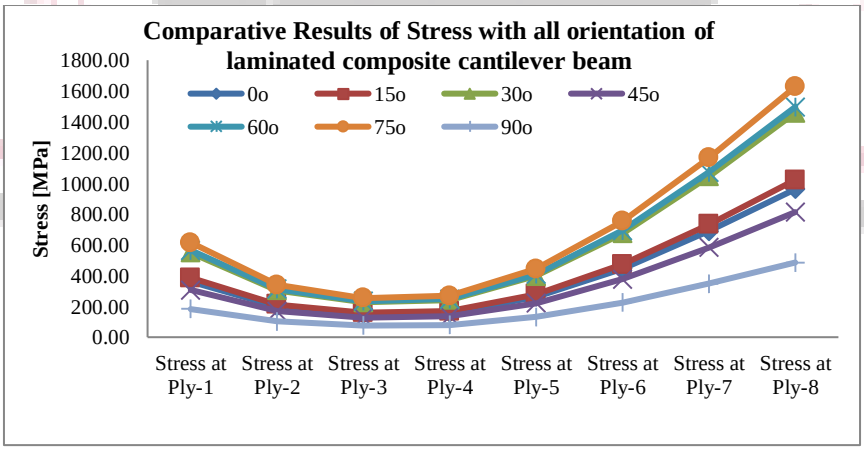

Figure 32 Comparative Results of Stress with all orientation of laminated composite cantilever beam

VI .CONCLUSION

In the present work the finite element analysis in order to investigate the stresses and the deformation in the laminates the composite cantilever beam with unidirectional (θ˚/θ˚/θ˚/θ˚) s and angle ply (θ˚/-θ˚/ θ˚/-θ˚) have been used to laminates the composite cantilever beam. Fiber orientation angle θ˚ is varied from 0˚, 15˚, 30˚, 45˚, 60˚, 75˚ and 90˚. A rectangular plate of 100 mm x 50 mm having central hole of 20 mm with total thickness of 1 mm fixed at the left side and the force of 1 KN on the right upper corner has been applied to check the stresses and deformation. For the creation of layer (ply)

ACP pre has been used in ansys workbench. The thickness of each layer is taken as 0.125 mm and total eight layers of boron-epoxy are used to make laminate. There are following conclusion have been observed from the above analysis.

- After performing structural analysis on rectangular laminates the composite cantilever beam at 1000 N applied in vertical direction for the ply orientation at 0º, the total deformation of 13.534 mm has been observed. the directional deformation of 0.1276 mm along the X- axis & the 1.0608 mm along the Y-axis has been observed and the maximum 961.32 MPa at 8th ply while the minimum stress of 149.73 MPa generated on the 3rd ply.
- For the ply orientation at 15º, the total deformation of 10.841 mm has been observed. the directional deformation of 0.0999 mm along the X- axis & the 0.7548 mm along the Y-axis has been observed and the maximum 1022.1MPa at 8th ply while the minimum stress of 159.2 MPa generated on the 3rd ply.
- For the ply orientation at 30º, the total deformation of 6.1906 mm has been observed, the directional deformation of 0.18459 mm along the X- axis & the 0.6765 mm along the Y-axis has been observed and the maximum 1458.2 MPa at 8th ply while the minimum stress of 227.12 MPa generated on the 3rd ply.
- For the ply orientation at 45º, the total deformation of 2.4722 mm has been observed, the directional deformation of 0.06267 mm along the X- axis & the 0.288 mm along the Y-axis has been observed and the maximum 812.72 MPa at 8th ply while the minimum stress of 126.59 MPa generated on the 3rd ply.
- For the ply orientation at 60º, the total deformation of 4.4071 mm has been observed, the directional deformation of 0.16354 mm along the X- axis & the 0.745 mm along the Y-axis has been observed and the maximum 1496.11 MPa at 8th ply while the minimum stress of 233.03 MPa generated on the 3rd ply.
- For the ply orientation at 75º, the total deformation of 27.567 mm has been observed, the directional deformation of 0.2 mm along the X- axis & the 1.026 mm along the Y-axis has been observed and the maximum 1627.1 MPa at 8th ply while the minimum stress of 253.43 MPa generated on the 3rd ply.
- For the ply orientation at 90º, the total deformation of 2.1932 mm has been observed, the directional deformation of 0.01826 mm along the X- axis & the 0.2253 mm along the Y-axis has been observed and the maximum 485.06 MPa at 8th ply while the minimum stress of 75.91 MPa generated on the 3rd ply.

From the above conclusion it has been observed that the stresses with all orientation of laminated composite cantilever beam, from ply 1 to ply 3 the stress value is decreasing for all orientation and from ply-3 to ply-8 it increasing, it also have been seen that the rectangular laminated composite cantilever beam having the minimum stress value for orientation angle 90º because in this case applied load is along the direction of fiber hence it can be concluded that according to the application of load direction orientation of ply can be make. So from the above analysis it can be stated that the ply orientation with 90º and 45º can be proposed.

References:

[1] Prombut P, Anakpotchanakul C. Deflection of Composite Cantilever Beams with a Constant I-Cross Section. IOP Conference Series: Materials Science and Engineering, vol. 501, Institute of Physics Publishing; 2019.

[2] Talekar N, Kotambkar M. Modal Analysis of Four Layered Composite Cantilever Beam with Lay-Up Sequence and Length-To-Thickness Ratio.Materials Today: Proceedings, vol. 21,Elsevier Ltd; 2020.

[3] Satheesh P, Reddy K, Bhargavi K, Nagaraju C. Tailoring of composite cantilever beam for maximum stiffness and minimum weight.IOSR Journal of Mechanical and Civil Engineering vol. 9. n.d. (2013)

[4] Malik S, Singh DK, Bansal G, Paliwal V, Manral AR. Finite element analysis of Euler's Bernoulli cantilever composite beam under uniformly distributed load at elevated temperature. Materials Today: Proceedings, vol. 46, Elsevier Ltd; 2021, p. 10725–31.

[5] Sayyad AS, Ghugal YM. Bending, buckling and free vibration of laminated composite and sandwich beams: A critical review of literature.Composite Structures, vol.171, Elsevier Ltd; 2017;171:486–504.

[6] Ahmed N, Mamun M, Ahmed A. Vibration Response Analysis of a Structural Metal Mild Steel under the Effect of Crack. IOP Conference Series: Materials Science and Engineering 2021;1092:012037.

[7] Elsheikh, A. Bistable Morphing Composites for Energy-Harvesting Applications. Polymers 2022, 14, 1893. [CrossRef]

[8] Chillara , V.S.C.; Dapino, M.J. Bistable Morphing Composites with Selectively-Prestressed Laminae. In Behavior and Mechanics of Multifunctional Materials and Composites 2017, Proceedings of the SPIE Smart Structures and Materials + Nondestructive Evaluation and Health Monitoring, Portland, OR, USA, 25–29 March 2017; SPIE: Bellingham, WA, USA, 2017; Volume 10165, p. 10165. [CrossRef]

[9] Sunil, B.R.; Reddy, G.P.K.; Patle, H.; Dumpala, R. Magnesium based surface metal matrix composites by friction stir processing. J. Magnes. Alloy. 2016, 4, 52–61. [CrossRef]

[10] Krishnan, R.; Pandiaraj, S.; Muthusamy, S.; Panchal, H.; Alsoufi, M.S.; Ibrahim, A.M.M.; Elsheikh, A. Biodegradable magnesium metal matrix composites for biomedical implants: Synthesis, mechanical performance, and corrosion behavior—A review. J. Mater. Res. Technol. 2022, 20, 650–670. [CrossRef]

[11]. AElsheikh, A.H.; Abd Elaziz, M.; Ramesh, B.; Egiza, M.; Al-qaness, M.A. Modeling of drilling process of GFRP composite using a hybrid random vector functional link network/parasitism-predation algorithm. J. Mater. Res. Technol. 2021, 14, 298–311. [CrossRef]

[12] Najjar, I.M.R.; Sadoun, A.M.; Abd Elaziz, M.; Abdallah, A.W.; Fathy, A.; Elsheikh, A.H. Predicting kerf quality characteristics in laser cutting of basalt fibers reinforced polymer composites using neural network and chimp optimization. Alex. Eng. J. 2022, 61, 11005–11018. [CrossRef]
[13] Showaib, E.A.; Elsheikh, A.H. Effect of surface preparation on the strength of vibration welded butt joint made from PBT composite. Polym. Test. 2020, 83, 106319. [CrossRef]
[14]Saleh Bassiouny, Jinghua Jiang, Aibin Ma, Dan Song, Yang Dong-hui,Effect of main parameters on the mechanical and wear behaviour of functionally graded materials by centrifugal casting: a review,Met. Mater. Int., 25 (2019), pp. 1395-1409, 10.1007/s12540-019-00273-8
[15] R. Fathi, A. Ma, B. Saleh, Q. Xu, J. Jiang,Investigation on mechanical properties and wear performance of functionally graded AZ91-SiCp composites via centrifugal castingMater. Today Commun., 24 (2020), 10.1016/j.mtcomm.2020.10116